ARTICLE
Journal of Cellular Biochemistry 106:279–284 (2009)

Journal of Cellular Biochemistry

A Transgenic Red Fluorescent Protein-Expressing Nude Mouse for Color-Coded Imaging of the Tumor Microenvironment

Meng Yang,[1] Jose Reynoso,[1] Michael Bouvet,[2] and Robert M. Hoffman[1,2*]

[1] *AntiCancer, Inc., 7917 Ostrow Street, San Diego, California 92111*

[2] *Department of Surgery, University of California San Diego, Moores UCSD Cancer Center, 3855 Health Sciences Drive, La Jolla, California 92093-0987*

ABSTRACT

The tumor microenvironment (TME) is critical for tumor growth and progression. We have previously developed color-coded imaging of the TME using a green fluorescent protein (GFP) transgenic nude mouse as a host. However, most donor sources of cell types appropriate for study in the TME are from mice expressing GFP. Therefore, a nude mouse expressing red fluorescent protein (RFP) would be an appropriate host for transplantation of GFP-expressing stromal cells as well as double-labeled cancer cells expressing GFP in the nucleus and RFP in the cytoplasm, thereby creating a three-color imaging model of the TME. The RFP nude mouse was obtained by crossing non-transgenic nude mice with the transgenic C57/B6 mouse in which the β-actin promoter drives RFP (DsRed2) expression in essentially all tissues. In crosses between nu/nu RFP male mice and nu/+ RFP female mice, the embryos fluoresced red. Approximately 50% of the offspring of these mice were RFP nude mice. In the RFP nude mouse, the organs all brightly expressed RFP, including the heart, lungs, spleen, pancreas, esophagus, stomach, duodenum, the male and female reproductive systems; brain and spinal cord; and the circulatory system, including the heart, and major arteries and veins. The skinned skeleton highly expressed RFP. The bone marrow and spleen cells were also RFP positive. GFP-expressing human cancer cell lines, including HCT-116-GFP colon cancer and MDA-MB-435-GFP breast cancer were orthotopically transplanted to the transgenic RFP nude mice. These human tumors grew extensively in the transgenic RFP nude mouse. Dual-color fluorescence imaging enabled visualization of human tumor–host interaction. The RFP nude mouse model should greatly expand our knowledge of the TME. J. Cell. Biochem. 106: 279–284, 2009.

KEY WORDS: RFP; GFP; TRANSGENIC; ORTHOTOPIC; MOUSE MODELS; MICROENVIRONMENT; STROMA; ANGIOGENESIS

The use of fluorescent proteins for imaging is revolutionizing in vivo biology [Hoffman, 2005, 2008]. Green fluorescent protein (GFP) has been shown to be able to be genetically linked with almost any protein providing a permanent and heritable label in live cells to study protein function and location. Many different colors of fluorescent proteins have now been produced in the laboratory or found in nature [Matz et al., 1999; Shaner et al., 2004]. With multiple colors, many processes can be visualized simultaneously in cells. Thus, live cells can be multiply labeled for imaging processes that heretofore could be seen only on fixed and stained cells.

Fluorescent protein imaging has been particularly useful to study tumor progression [Hoffman, 2005]. With the use of multiple-colored-proteins, we developed imaging of the tumor microenvironment (TME) by color-coding tumor and stromal cells. The TME is critical for tumor growth and progression. Indeed, cancer cells and stromal cells must replicate in parallel in order for the tumor to grow. Our initial color-coded imaging technology of the TME used a GFP transgenic nude mouse as a host in which we transplanted dual-color cancer cells expressing GFP in the nucleus and red fluorescent protein (RFP) in the cytoplasma [Yang et al., 2003, 2004; Yamamoto et al., 2004]. However, most donor sources of stromal cell types, appropriate for study in the TME, are from mice expressing GFP. Therefore, a nude mouse expressing RFP would be an appropriate host for transplantation of GFP-expressing stromal cells.

RFP (DsRed) had displayed toxicity in murine embryos, which hampered development of an RFP transgenic mouse. However, Nagy's group developed an RFP variant, DsRed.T3, enabling them to produce a transgenic RFP mouse [Vintersten et al., 2004].

Grant sponsor: National Institutes of Health; Grant number: CA109949; Grant sponsor: American Cancer Society; Grant number: RSG-05-037-01-CCE; Grant sponsor: National Cancer Institute; Grant number: CA103563.

*Correspondence to: Robert M. Hoffman, 7917 Ostrow Street, San Diego, CA 92111. E-mail: all@anticancer.com

Received 20 October 2008; Accepted 22 October 2008 • DOI 10.1002/jcb.21999 • 2008 Wiley-Liss, Inc.
Published online 18 December 2008 in Wiley InterScience (www.interscience.wiley.com).

In this study using the transgenic RFP mouse described by Nagy's group [Vintersten et al., 2004], we developed a transgenic RFP nude mouse that could serve as a host for GFP or GFP-RFP labeled human cancer cells. We report here the development and characterization of this transgenic RFP nude mouse which has ubiquitous RFP expression. The RFP nude mouse was used to visualize the growth, metastasis, and tumor–host interaction of human tumor cell lines expressing GFP or GFP and RFP.

MATERIALS AND METHODS

TRANSGENIC RED FLUORESCENT PROTEIN NUDE MICE

Transgenic C57/B6-RFP mice were obtained from Jackson Labs (Bar Harbor, ME). C57/B6-RFP mice expressed the RFP (DsREDT3) under the control of a chicken beta-actin promoter and cytomegalovirus enhancer. All of the tissues from this transgenic line, with the exception of erythrocytes, were red under blue excitation light. Six-week-old transgenic RFP female mice were crossed with both 6–8-week-old BALB/c nu/nu and NCR nu/nu male mice (Harlan, Indianapolis, IN), respectively. Male F1 fluorescent nude mice were crossed with female F1 immunocompetent RFP mice. When female F2 immunocompetent RFP mice were crossed with male RFP nude or using F2 RFP nude male to back cross with female F1 immunocompetent RFP mice, approximately 50% of their offspring were RFP nude mice. RFP nude mice were then consistently produced using the methods described above.

GFP AND DUAL-COLOR CANCER CELLS

GFP and dual-color cancer cells expressing GFP in the nucleus and RFP in the cytoplasm, which were previously developed in our laboratory [Yamamoto et al., 2004], were used in the study.

GFP-EXPRESSING ORTHOTOPIC BREAST CANCER—RFP-HOST MODEL

Six-week-old female nude RFP mouse was injected orthotopically with a single dose of 10^6 GFP-expressing MDA MB435-GFP cells. Cells were first harvested by trypsinization and washed three times with cold serum-containing medium, then kept on ice. Cells were injected in the mammary fat pads of the animal in a total volume of 30 μl within 40 min of harvesting.

GFP-EXPRESSING ORTHOTOPIC HUMAN COLON CANCER—RFP-HOST MODEL

Six-week-old male RFP nude mice, was injected orthotopically with a single dose of 1×10^6 GFP-expressing HCT 116 human colon cancer cells. Cells were first harvested by trypsinization and washed three times with cold serum-containing medium, then kept on ice. The cells were injected within 40 min of harvesting. After proper exposure of the colon through a lower abdominal incision, the cells were injected into the wall of colon in a total volume of 30 μl. The incision in the abdominal wall was closed with a 6–0 surgical suture in one layer.

GFP-RFP EXPRESSING ORTHOTOPIC B16F10 MOUSE MELANOMA—RFP-HOST MODEL

Six-week-old male RFP nude mice, was injected subdermally with a single dose of dual-color 1×10^6 GFP-RFP-expressing B16F10 mouse melanoma cancer cells in a total volume of 30 μl. Cells were first harvested by trypsinization and washed three times with cold serum-containing medium, then kept on ice. The cells were injected subdermally within 40 min of harvesting.

GFP-RFP EXPRESSING ORTHOTOPIC PC-3 HUMAN PROSTATE CANCER—RFP-HOST MODEL

Six-week-old male RFP nude mice, was injected in the prostate with a single dose of 1×10^6 GFP-expressing PC-3 human prostate cancer cells. Cells were first harvested by trypsinization and washed three times with cold serum-containing medium, then kept on ice. The cells were injected within 40 min of harvesting. After proper exposure of the prostate through a lower abdominal incision, the cells were injected into the prostate in a total volume of 30 μl. The incision in the abdominal wall was closed with a 6–0 surgical suture in one layer.

IMAGING

The following imaging systems were used in this study: the Hamamatsu C5810 three-chip CCD camera (Hamamatsu Photonics, Hamamatsu, Japan); the Olympus IMT-2 inverted fluorescence microscope (Olympus Corp., Tokyo, Japan); the FluorVivo imaging system (Indec Biosystems, Santa Clara, CA); and the Olympus IV100 intravital scanning laser microscope (Olympus Corp., Tokyo, Japan).

RESULTS AND DISCUSSION

DEVELOPMENT OF A TRANSGENIC RFP NUDE MOUSE

We have developed the RFP nude mouse, a new strain of transgenic nude mice, by crossing non-transgenic nude mice with the transgenic-RFP C57/B6 mouse (Fig. 1).

THE RFP NUDE MOUSE EXPRESSES RFP ESSENTIALLY IN ALL TISSUES

After sacrifice of the RFP transgenic nude mouse, organs including brain, heart and lungs, liver, the circulatory system, uterus and ovary, pancreas, kidney, and spleen were harvested, and imaged with the FluorVivo imaging system. All of the tissues from this transgenic line, with the exception of erythrocytes, were red fluorescent under appropriate excitation light (Fig. 2).

WHOLE-BODY IMAGING OF CANCER CELLS LABELED WITH GFP ORTHOTOPICALLY TRANSPLANTED IN RFP NUDE MICE

GFP-expressing human cancer cell lines, including HCT116-GFP human colon and MDA-MB-435-GFP human breast were orthotopically transplanted in the RFP nude mice. The GFP-expressing tumors were non-invasively imaged with the FluorVivo imaging system. These human tumors had similar growth rate with that of the tumors growing in the non-transgenic nude mouse (Fig. 3).

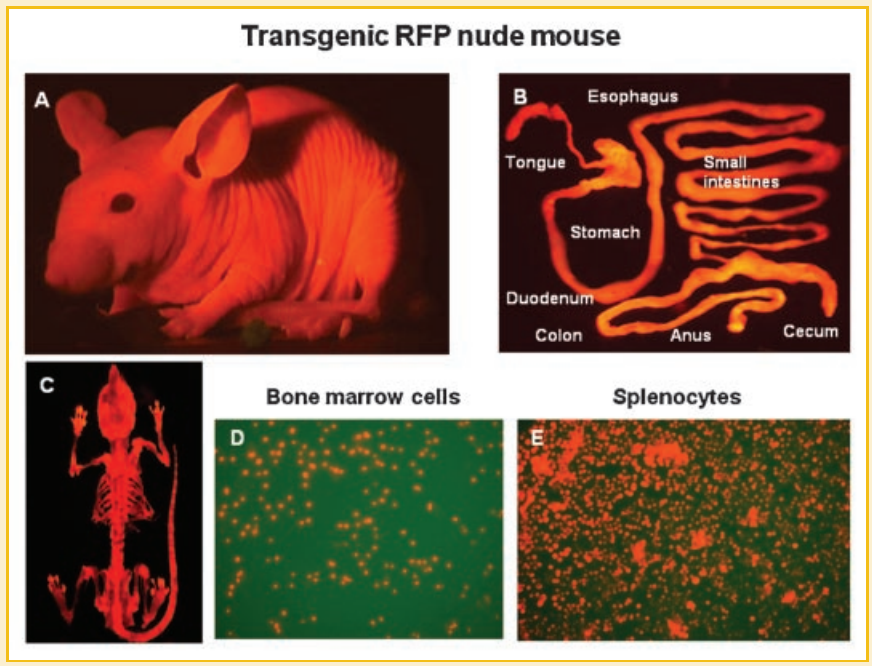

Fig. 1. Transgenic RFP nude mouse. A: Whole-body image of transgenic RFP nude mouse. B: Digestive tract of RFP nude mice. C: Whole skeleton of RFP nude mouse. D: Bone marrow cells of the RFP nude mouse. E: Splenocytes of the RFP nude mouse. Images were taken with a Hamamatsu C5810 tree-chip CCD camera (A) and an Olympus IMT-2 inversed fluorescence microscope (B–E).

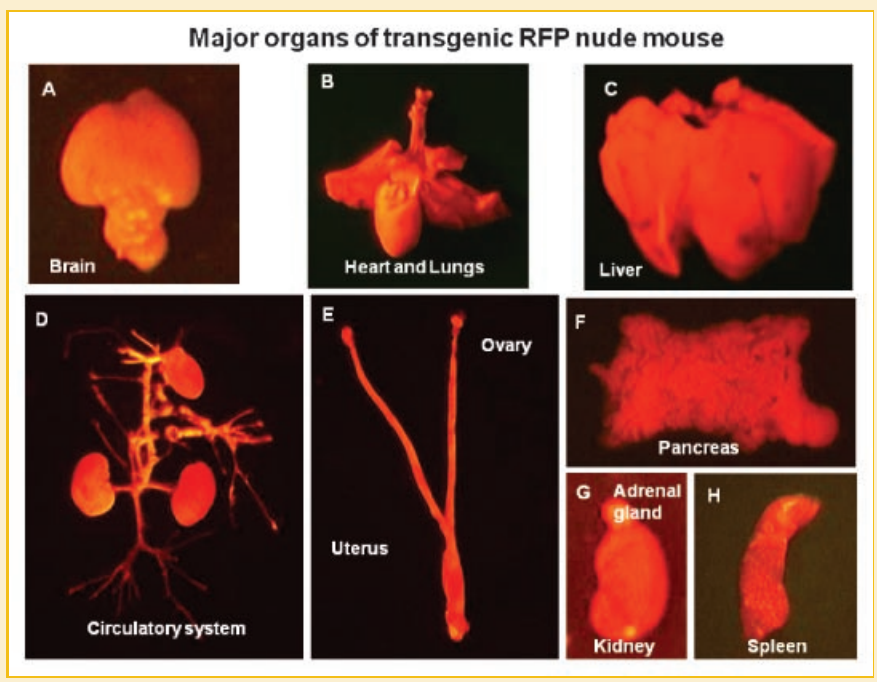

Fig. 2. Major organs of transgenic RFP nude mouse. All of the major organs and tissues are red under fluorescence excitation with blue light. A: Brain. B: Heart and Lungs. C: Liver. D: Circulatory system. E: Uterus and ovary. F: Pancreas. G: Kidney and adrenal gland. H: Spleen. All images were taken with the Indec Biosystems FluorVivo imaging system.

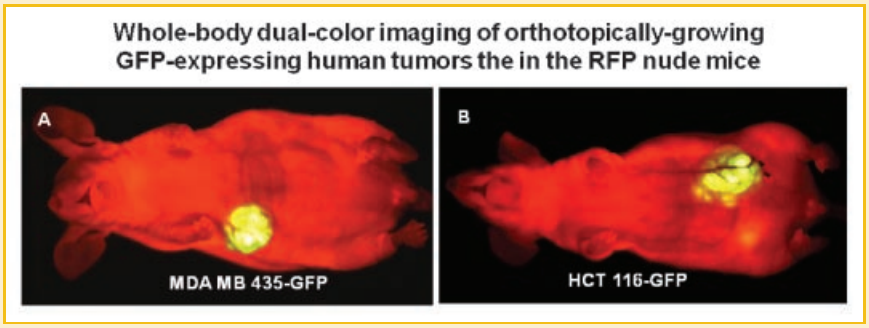

Fig. 3. Whole-body dual-color imaging of orthotopically growing GFP-expressing human tumors in the RFP nude mice. A: Whole-body image shows the GFP-expressing MDA-MB-435 human mammary cancer growing orthotopically in the RFP nude mouse 4 weeks after implantation. B: Whole-body image shows the GFP-expressing HCT116-RFP human colon cancer growing orthotopically in the RFP nude mouse 4 weeks after implantation. All images were taken with the Indec FluorVivo imaging system.

TUMOR–HOST INTERACTION AND TUMOR MICROENVIRONMENT (TME)

Dual-color fluorescence imaging enabled visualization of PC-3-GFP human prostate (Fig. 4A,B) and the B16F10 mouse melanoma expressing GFP in the nucleus and RFP in the cytoplasm, interacting with RFP-expressing host cells (Fig. 4C,D). RFP-expressing tumor vasculature in viable tumor tissue and necrotic tumor tissue in the same tumor mass were visualized (Fig. 4A). RFP-expressing tumor vasculature can be readily identified in the area where the tumor tissue maintained good viability. However, only remnants of RFP-expressing vasculature could be visualized in the necrotic area. GFP-expressing PC-3 cancer cells were visualized in the lung of RFP nude mouse 8 weeks after tumor implantation (Fig. 4B). Numerous dying B16F10-dual-color melanoma cancer cells can be visualized in the area where the tumor vasculature is lacking (Fig. 4C). Numerous well-developed, host-derived RFP-expressing blood vessels were visualized in the GFP-expressing mouse melanoma 2 weeks after subcutaneous injection of B16F10-dual-color melanoma cells in the transgenic RFP mouse (Fig. 4D).

Fluorescent proteins have revolutionized biological science. GFP has been shown to be able to be genetically linked with almost any protein providing a permanent and heritable label in live cells to

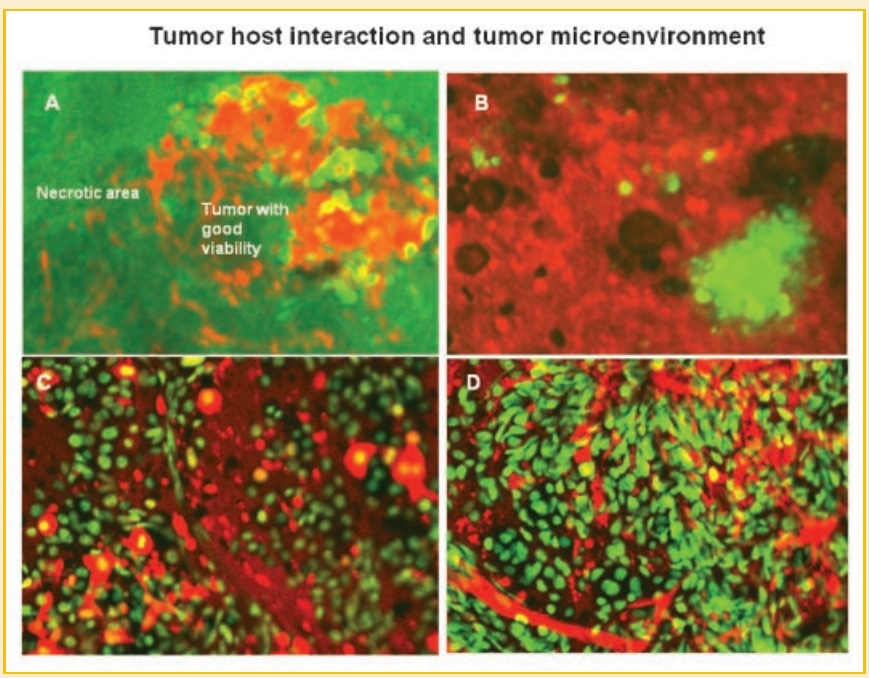

Fig. 4. Tumor–host interaction and tumor microenvironment. A: Tumor vasculature in viable GFP-expressing PC-3 tumor tissue and necrotic tumor tissue in the same tumor mass. RFP-expressing tumor vasculature can be readily identified in the area where the tumor tissue maintained good viability. However, only remnants of RFP-expressing vasculature can be visualized in the necrotic area. B: GFP-expressing PC-3 cancer cells can be visualized in the lung of RFP nude mouse 8 weeks after tumor implantation. C: Numerous dying B16F10-dual-color melanoma cells can be visualized in the footpad in the area the tumor vasculature is lacking. D: Numerous well-developed, host-derived RFP-expressing blood vessels were visualized in the footpad in the GFP-expressing mouse melanoma 2 weeks after subcutaneous injection of B16F10-dual-color melanoma cells in the transgenic RFP mouse. Images were taken with the Olympus IV100 intravital scanning microscope using tumor tissue obtained from the footpad.

study protein function and location. Many different colors of fluorescent proteins have now been produced in the laboratory or found in nature [Matz et al., 1999; Shaner et al., 2004]. With multiple colors, many processes can be visualized simultaneously in cells. Thus, cells can be multiply labeled for live imaging of processes that heretofore could be seen only on fixed and stained cells. What previously was invisible can now be seen in real-time in living cells expressing fluorescent proteins. Our laboratory pioneered the use of fluorescent proteins for imaging in mice from macro to sub-cellular [Chishima et al., 1997; Yang et al., 2000; Hoffman, 2005; Hoffman and Yang, 2006a,b,c].

Whole-body, non-invasive imaging with fluorescent proteins depends in large part on the brightness of the protein. Whole-body imaging with fluorescent proteins has been shown to be able to quantitatively track tumor growth and metastasis, gene expression, angiogenesis, and bacterial infection [Zhao et al., 2001; Hoffman, 2005] even at sub-cellular resolution depending on the position of the cells in the animal. Interference by skin autofluorescence is kept to a minimum with the use of proper filters. Very simple equipment such as an LED flashlight with a narrow-band filter and a bandpass emission filter can be used to whole-body image mice implanted with cells expressing fluorescent proteins [Yang et al., 2005].

The features of fluorescent-protein-based imaging, such as a very strong and stable signal enable non-invasive whole-body imaging down to the sub-cellular level [Yang et al., 2007] make fluorescent-protein imaging, especially with red-shifted proteins, far superior to luciferase-based imaging. Luciferase-based imaging, with its very weak signal [Ray et al., 2004], precluding image acquisition and allowing only photon counting with pseudocolor-generated images, has very limited applications [Hoffman, 2005]. For example, cellular imaging in vivo is not possible with luciferase. The dependence on circulating luciferin makes the signal from luciferase imaging unstable [Burgos et al., 2003; Hoffman and Yang, 2006c]. The one possible advantage of luciferase-based imaging is that no excitation light is necessary. However, far-red absorbing proteins such as Katushka greatly reduce any problems with excitation, even in deep tissues, as shown by Shcherbo et al. [2007].

A triple fusion reporter vector harboring a *Renilla* luciferase reporter gene, a reporter gene encoding a monomeric RFP, and a mutant herpes simplex virus type thymidine kinase were tested in vivo. A highly sensitive cooled CCD camera that is compatible with both luciferase and fluorescence imaging compared these two signals from the fused reporter gene using a lentivirus vector in 293T cells implanted in nude mice. The signal from RFP was found to be ~1,000 times stronger than the signal from luciferase [Ray et al., 2004]. The weak signal from luciferase necessitates photon counting, with the construction of a pseudo-image in vivo rather than true imaging, therefore greatly reducing resolution and precluding the in vivo cellular imaging that is an important feature of fluorescent-protein imaging. In addition, the rapid clearance of the injected luciferase results in an unstable signal that makes comparison of data difficult [Burgos et al., 2003]. The stronger signals from fluorescent proteins allow much more cost-efficient instrumentation. To overcome limits on fluorescent protein imaging imposed by the skin, reversible skin-flap window models have been developed that allow single-cell imaging on most organs of the mouse [Yang et al., 2002].

Red-emitting fluorescent proteins were first described in the late 1990s. The first such protein was isolated and cloned from the coral *Discosoma sp*. obtained from an aquarium in Moscow [Matz et al., 1999] and termed Ds-Red. After extensive modification by mutagenesis, a very bright red protein was eventually isolated, termed DsRed-2 with an emission wavelength peak of 588. DsRed-2 has shown to be very enabling for whole-body imaging and has been used to non-invasively follow cancer metastasis in real-time [Katz et al., 2003] in nude mice as well as whole-body image dual-color models of tumors expressing DsRed-2 growing in transgenic GFP nude mice as hosts [Yang et al., 2003].

In 2004, a report appeared [Shaner et al., 2004] describing a series of red-shifted proteins obtained by mutating DsRed. These proteins, termed mCherry, mRaspberry, mPlum, and mTomato, had emission maxima as long as 649 nm. However, these mutants have low quantum yields, thereby reducing their brightness.

A very bright, red-shifted variant has now been isolated with an excitation peak at 588 mm and emission peak at 635 nm both of which are relatively non-absorbed by issues and homoglobin. After four cycles of random mutagenesis and further selection for a bright, far-red-shifted protein, a protein named Katushka, was isolated. Katushka has many favorable properties in addition to its absorption and emission peaks including a rapid maturation time of 20 min. Importantly, an extinction coefficient of 65,000 $M^{-1}cm^{-1}$ and quantum yield of 0.34, make Katushka the brightest fluorescent protein with an emission maximum beyond 620 nm [Shcherbo et al., 2007].

The transgenic mice used in the present study were constructed with a variant of DsRed (DsRedT3) [Vintersten et al., 2004].

Cancer cells coexist in a complex association with host-stromal tissue cells in the TME. The stroma provides the vascular supply to the tumor in the angiogenesis process as well as many other cell types and functions. The factors that regulate the development of the stromal elements, as well as the influences these constituents have on the tumor, are poorly understood. The lack of information about the interaction between cancer cells and stroma can be attributed in part to lack of suitable models [Folkman, 2003]. Tumor progression is a multistep process accompanied by the accumulation of mutations and altered chromosomes (aneuploidy) in cancer cells. However, it is now becoming clear that the TME is also critical for malignancy, which is in part the product of interaction between different cancer and host cell types [Paget, 1889].

The heterogeneous and structurally complex nature of the interactive TME is little understood. The relative amount of stroma and its composition vary considerably from tumor to tumor and vary within a tumor over the course of tumor progression. The interaction between cancer cells and stromal cells largely determines the phenotype of the tumor. For example, recent studies have shown that the growth, invasiveness, and angiogenesis of human breast tumor xenografts in mice depend on the presence of stromal fibroblasts [Orimo et al., 2005].

The TME is a potential therapeutic target. Advantages to targeting the stroma cells are that the cells are genetically stable unlike cancer cells and are therefore less likely to develop drug resistance [Kerbel,

1997; Ferrara and Kerbel, 2005]. For example, anti-vascular endothelial growth factor antibodies, which inhibit formation of new blood vessels in the tumor, are used to treat colorectal cancer [Chen et al., 2006].

In our previous study, three-color whole-body imaging of the two-color cancer cells were implanted in a GFP-expressing transgenic nude mouse. Various in vivo phenomena of tumor–host interaction and cellular dynamics were imaged, including stromal cells intimately interacting with the cancer cells, tumor vasculature, and tumor blood flow [Yang et al., 2007].

The RFP mouse described in the present report opens many new possibilities for studying the TME by adding the possibility of adding GFP stromal cells. The RFP nude mouse model as described herein should yield important new information on the TME.

ACKNOWLEDGMENTS

This work was supported in part by grants from the National Institutes of Health (CA109949), and American Cancer Society (RSG-05-037-01-CCE) to MB and the National Cancer Institute grant CA103563 (to AntiCancer, Inc.).

REFERENCES

Burgos JS, Rosol M, Moats RA, Khankaldyyan V, Kohn DB, Nelson MD, Jr., Laug WE. 2003. Time course of bioluminescent signal in orthotopic and heterotopic brain tumors in nude mice. Biotechniques 34:1184–1188.

Chen HX, Mooney M, Boron M, Vena D, Mosby K, Grochow L, Jaffe C, Rubinstein L, Zwiebel J, Kaplan RS. 2006. Phase II multicenter trial of bevacizumab plus fluorouracil and leucovorin in patients with advanced refractory colorectal cancer: An NCI Treatment Referral Center Trial TRC-0301. J Clin Oncol 24:3354–3360.

Chishima T, Miyagi Y, Wang X, Yamaoka H, Shimada H, Moossa AR, Hoffman RM. 1997. Cancer invasion and micrometastasis visualized in live tissue by green fluorescent protein expression. Cancer Res 57:2042–2047.

Ferrara N, Kerbel RS. 2005. Angiogenesis as a therapeutic target. Nature 438:967–974.

Folkman J. 2003. Angiogenesis and apoptosis. Semin Cancer Biol 13:159–167.

Hoffman RM. 2005. The multiple uses of fluorescent proteins to visualize cancer in vivo. Nat Rev Cancer 5:796–806.

Hoffman RM. 2008. A better fluorescent protein for whole-body imaging. Trends Biotechnol 26:1–4.

Hoffman RM, Yang M. 2006a. Subcellular imaging in the live mouse. Nat Protoc 1:775–782.

Hoffman RM, Yang M. 2006b. Color-coded fluorescence imaging of tumor–host interactions. Nat Protoc 1:928–935.

Hoffman RM, Yang M. 2006c. Whole-body imaging with fluorescent proteins. Nat Protoc 1:1429–1438.

Katz MH, Takimoto S, Spivak D, Moossa AR, Hoffman RM, Bouvet M. 2003. A novel red fluorescent protein orthotopic pancreatic cancer model for the preclinical evaluation of chemotherapeutics. J Surg Res 113:151–160.

Kerbel RS. 1997. A cancer therapy resistant to resistance. Nature 390:335–336.

Matz MV, Fradkov AF, Labas YA, Savitsky AP, Zaraisky AG, Markelov ML, Lukyanov SA. 1999. Fluorescent proteins from non-bioluminescent Anthozoa species. Nat Biotechnol 17:969–973.

Orimo A, Gupta PB, Sgroi DC, Arenzana-Seisdedos F, Delaunay T, Naeem R, Carey VJ, Richardson AL, Weinberg RA. 2005. Stromal fibroblasts present in invasive human breast carcinomas promote tumor growth and angiogenesis through elevated SDF-1/CXCL12 secretion. Cell 121:335–348.

Paget S. 1889. The distribution of secondary growths in cancer of the breast. Lancet 133:571–573.

Ray P, De A, Min JJ, Tsien RY, Gambhir SS. 2004. Imaging tri-fusion multimodality reporter gene expression in living subjects. Cancer Res 64:1323–1330.

Shaner NC, Campbell RE, Steinbach PA, Giepmans BN, Palmer AE, Tsien RY. 2004. Improved monomeric red, orange, and yellow fluorescent proteins derived from Discosoma sp. red fluorescent protein. Nat Biotechnol 22:1567–1572.

Shcherbo D, Merzlyak EM, Chepurnykh TV, Fradkov AF, Ermakova GV, Solovieva EA, Lukyanov KA, Bogdanova EA, Zaraisky AG, Lukyanov S, Chudakov DM. 2007. Bright far-red fluorescent protein for whole-body imaging. Nat Methods 4:741–746.

Vintersten K, Monetti C, Gertsenstein M, Zhang P, Laszlo L, Biechele S, Nagy A. 2004. Mouse in red: Red fluorescent protein expression in mouse ES cells, embryos, and adult animals. Genesis 40:241–246.

Yamamoto N, Jiang P, Yang M, Xu M, Yamauchi K, Tsuchiya H, Tomita K, Wahl GM, Moossa AR, Hoffman RM. 2004. Cellular dynamics visualized in live cells in vitro and in vivo by differential dual-color nuclear-cytoplasmic fluorescent-protein expression. Cancer Res 64:4251–4256.

Yang M, Baranov E, Jiang P, Sun F-X, Li X-M, Li L, Hasegawa S, Bouvet M, Al-Tuwaijri M, Chishima T, Shimada H, Moossa AR, Penman S, Hoffman RM. 2000. Whole-body optical imaging of green fluorescent protein-expressing tumors and metastases. Proc Natl Acad Sci USA 97:1206–1211.

Yang M, Baranov E, Wang J-W, Jiang P, Wang X, Sun F-X, Bouvet M, Moossa AR, Penman S, Hoffman RM. 2002. Direct external imaging of nascent cancer, tumor progression, angiogenesis, and metastasis on internal organs in the fluorescent orthotopic model. Proc Natl Acad Sci USA 99:3824–3829.

Yang M, Li L, Jiang P, Moossa AR, Penman S, Hoffman RM. 2003. Dual-color fluorescence imaging distinguishes tumor cells from induced host angiogenic vessels and stromal cells. Proc Natl Acad Sci USA 100:14259–14262.

Yang M, Reynoso J, Jiang P, Li L, Moossa AR, Hoffman RM. 2004. Transgenic nude mouse with ubiquitous green fluorescent protein expression as a host for human tumors. Cancer Res 64:8651–8656.

Yang M, Luiken G, Baranov E, Hoffman RM. 2005. Facile whole-body imaging of internal fluorescent tumors in mice with an LED flashlight. BioTechniques 39:170–172.

Yang M, Jiang P, Hoffman RM. 2007. Whole-body subcellular multicolor imaging of tumor–host interaction and drug response in real-time. Cancer Res 67:5195–5200.

Zhao M, Yang M, Baranov E, Wang X, Penman S, Moossa AR, Hoffman RM. 2001. Spatial-temporal imaging of bacterial infection and antibiotic response in intact animals. Proc Natl Acad Sci USA 98:9814–9818.